Mechanical propertiesof monolayerh-BN sheet under in-plane shear displacement

Y. Tian[1], Z. Li[1], K. Cai[1], F. Wang[1], D. Zhang[1], B. Shirinzadeh[2], S. Fatikow[3]

[1]Key Laboratory of Mechanism Theory and Equipment Design of Ministry of Education, Tianjin University, Tianjin 300072, China

[2]Robotics and Mechatronics Research Laboratory, Department of Mechanical and Aerospace Engineering, Monash University, Clayton VIC 3800, Australia

[3]Division of Microrobotics and Control Engineering, University of Oldenburg, 26111 Oldenburg, Germany

Abstract: The mechanical properties including wrinkling patterns and fracture behavior of the monolayer h-BN sheets have been investigated using classic molecular dynamics simulations and continuum model. The wrinkling pattern formation and evolutionhave been firstly explored. The dependences of the wrinkling shape, amplitude and wavelength,as well as wrinkling number on shear displacement are extensively elucidated. The influences of geometry and shear load direction as well as temperature on the fracture behavior have also been studied to obtain further insights into the properties of the monolayer h-BN sheet.

Keywords: h-BN sheet, wrinkling, molecular dynamics, mechanical property, shear displacement.

1. Introduction

Graphene sheet is an ideal monolayer two-dimensionalgraphite crystal with only a carbon atom thickness[1]. The advent of graphene sheet has attracted research interests all over the world. Meanwhile, recent research attentions to graphene sheet have brought the spotlight to its analogue two-dimensional material of hexagonal boron nitride, h-BN sheet, in which C atoms are fully substituted with equal alternating B and N atoms. Since the masses of B and N atoms approach that of C atom, and the B-N bond length is very close to C-C bond length, so h-BN sheet has a similar lattice structure and parameters to graphemesheet[2,3]. Unlike graphene sheet, h-BN sheet does not absorb light in the visible region of the electromagnetic spectrum, and thus it is also called white graphene sheet. Recently, h-BN sheet is considered as one of the most promising inorganic nanosytemsto be explored[4]. Compared with the graphene, h-BN sheet has a number of advantages including: high thermal conductivity[5], superb electronic and magnetic character[6], wide optical bandgap[7], small friction coefficient[8-10], ultraviolet light emission[11], and thus it hasgreatly potential usages in the scientific engineering fields such as nano-sensing and measurement [12], nano tribology and luburication[13,14]. Further investigations have been directed towards this kind of h-BN sheet to explore the physical, chemical, and electric characteristics. It is found that h-BN sheet can be used as a highly effective insulator in graphene-based electronics,and that may help graphene supplant the silicon[15]. h-BN sheet has also exhibitedsuperhydrophobicity[16-20], which can be used as self-cleaning materials. Lei et al. [21]shows that h-BN sheet can preferentially soak up organic pollutants such as chemicals or engine oil, and it is easier to clean and re-use than graphene sheet, which is such a gratifying discovery.In addition, h-BN sheet possesses much higher chemical and thermal stability than its graphitic counterpart.

Wrinkling is an intrinsic feature of ultra-thinsheets includinggraphene and h-BN sheet. The

wrinkles are easily observed in ultra-thin sheets owing to those relatively small bending rigidity. The spontaneous wrinkles in graphene sheets were first discovered by Meyer et al. in 2007[22]. The existence of wrinkles is the fundamental reason why the graphene sheet can be stable in the form of the two-dimensional structure. Based on principle of wrinkling, we can form different folding graphene structures, such as nanotubes[23] and nanoribbons[24], and different folding methods may transform them to complex shapes with new and distinct properties[25]. Thus, wrinkling property is one of the crucial issues of such kinds of nano-sheet to be extensively explored. Those wrinkles can be obtained by various external loads. Wang [26] utilized an indenter trip tip of diameter 0.535nm to press the center of a circular graphene sheet of radius 16nm. That load can be reasonably regarded as a point load because the size of indenter is too small for the graphene sheet. The graphene sheet has some strip-like wrinkles shape along the circumference of the circle.Bao[27] observed the wrinkling of graphene sheets subjected to thermal load. Because two-dimensional structured graphene sheets have a negative thermal expansion coefficient, so that thermal load is equivalent to an in-plane tension stress.Duan [28] investigated the initiation and development of wrinkles in a monolayergraphene subjected to in plane shear displacement. The relationship between the wavelength and amplitude of wrinkles and the applied shear displacements has been established. Zhang [29] explored the wrinkling phenomenon in an annular graphene under circular shearing at the inner edge. It is also confirmed that the wrinkle profile in terms of wave amplitude and wavelength depends on the magnitude of the circular shearing. The obtained advanced knowledge paves the way for the potential applications of monolayergraphene in the development of nano fluidic electronics, and nano-biological science. However, there are seldom research efforts dedicated to the h BN sheet, which is also an urgent issue to be explored for its perspective applications.

In this paper, the wrinkling phenomenon in a monolayer h-BN sheet subjected to in-plane shear load has been systematically explored through molecular dynamics (MD) simulation. The dependences of the wavelength and amplitude of wrinkles, as well as the energy and stress with the shear displacement have been investigated. The continuum plate model has been developed and utilized to validate the MD computational analyses.The size effects ofmonolayer h-BN sheet on the energy and stress have been studied to obtain further insight into the wrinkling characteristics of such kinds of nano-sheets.In addition, the influences of the load directionand temperature on the fracture behavior have also been provided.

2. Computational methodologies

2.1 MD simulations

During the practical applications of monolayer h-BN sheet, it is usually cut into fragments and thus sheet edges are generated. It is demonstrated that thechirality of edges seriously affect the physical properties of the monolayer sheets [30]. There aregenerally two types of sheet edges: armchair edge and zigzagedge asshown in Fig.1.For a rectangular sheet, there are two armchair edges and two zigzag edges located at opposite sides. In order to investigate the wrinkling phenomenon of h-BN sheet with consideration of the edge effects, the shear displacements are chosen along the armchair and zigzag directions, respectively.

Molecular dynamics simulations are performed using Large-scale Atomic/Molecular Massively Parallel Simulator (LAMMPS).The MD simulation model is shown in Fig. 2.To compute the shear properties of h-BN sheets,a total of 2760 atoms with a size of 14.94nm×4.93 nm are used for simulation. The B-N bond length is 0.145 nm. The two long edges of the h-BN sheet are fixedwhile the other two sideedges are free of constrains. Then the entire h-BN is initially relaxed using NVTensemble until the energy of the system is fully minimized.NVTensemblemeans the

number of atoms, volume, and temperature keep constant. In order to reduce the thermal vibration of h-BNsheet as much as possible, the simulation temperature is controlled at around 1k using the Andersen thermostat temperature control methodology. After relaxation of the entire system, the upper side of the monolayer h-BN sheet is subjected to the shear displacement with the rate of 0.01nm/ps, while the bottom side is fixed and other two sides is free. Thus, the wrinkling behavior of the monolayer h-BN sheet can be investigated.

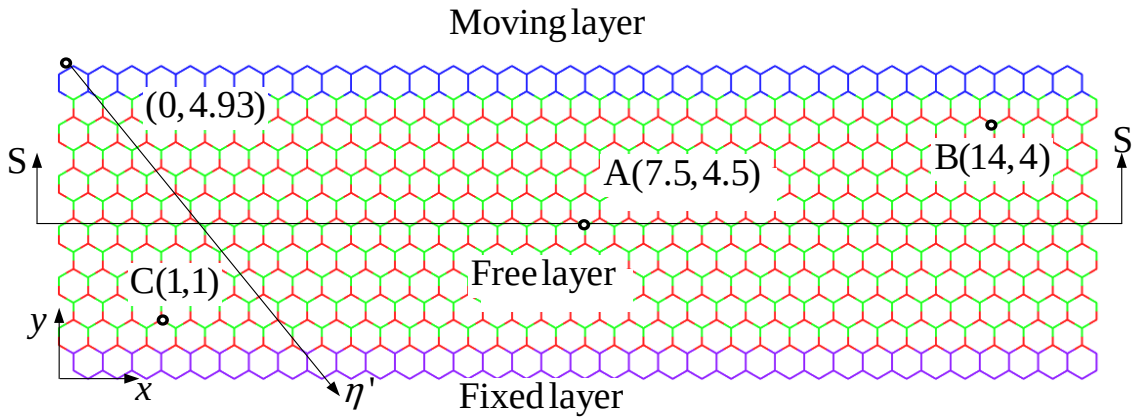

Fig. 1 Atomic model of monolayerh-BN sheet

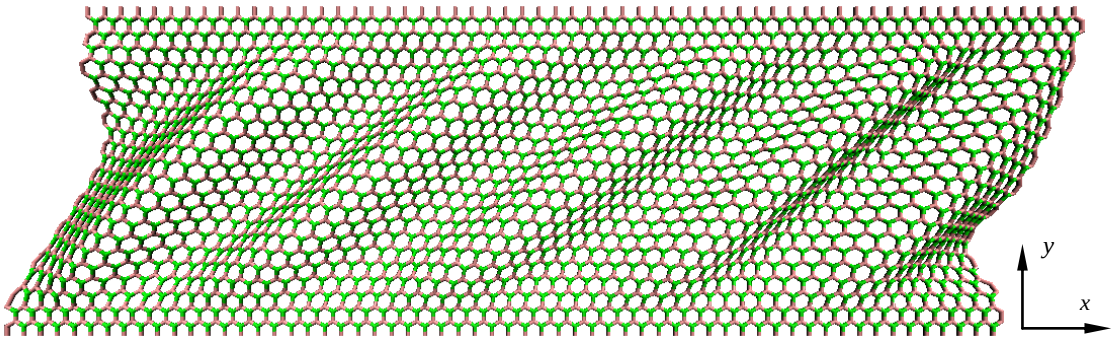

Fig. 2 A rectangular h-BN sheet subjected to a shear displacement of 1.2nm. The length and width grapheme/BN sheet are 14.94 nm and 4.93 nm.

2.2 Continuum modelling

In order to establish the analytical wrinkling model of the monolayer h-BN sheet, a plane rectangular membrane structure is considered and the coordinate frame *xoy*also established as shown in Fig. 3, where *L*, *H* and *t* are the length, width and thickness of the plane, respectively,*E*

and ν are the elasticity modulus and Poisson's ratio, respectively. The bottom side is completely fixed, andthe top side moves along the load direction.When the top side moves tothe shear displacement δ,the plane will generate wrinkles under the effect of the shear strain. The uniform wrinkles in the central region are taken into considered. Since the wrinkles are aligned with the directionseparated45°from x axis, the local coordinate frame $\xi o\eta$ is established with the axis ξalong the wrinkle direction, and axis ηperpendicular toaxisξ. Based on the established geometric model, the local wrinkles can be theoretically analyzed using continuum shell theory. The partial view of one wrinkle is shown in Fig. 4,where σ_{ξ} and σ_{η} are the stresses in $\xi$and ηdirections.

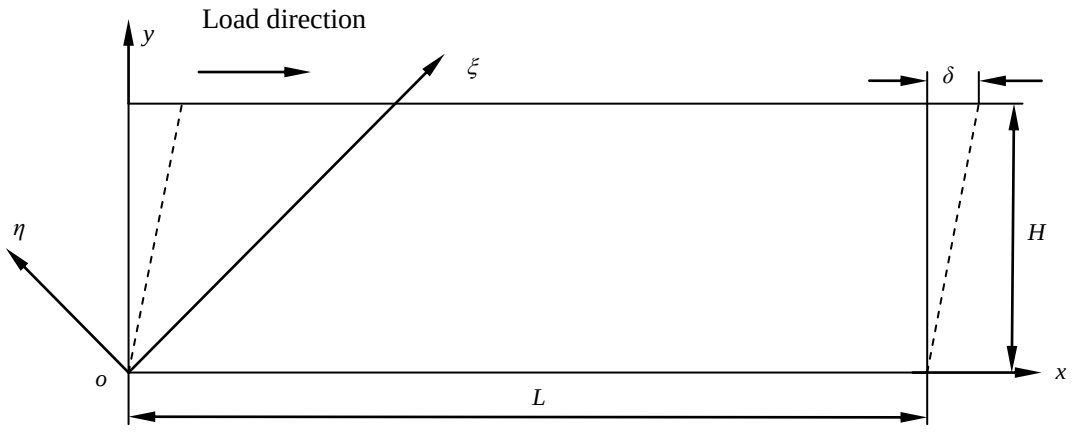

Fig. 3Rectangular continuum subjected in-plane horizontal shear load

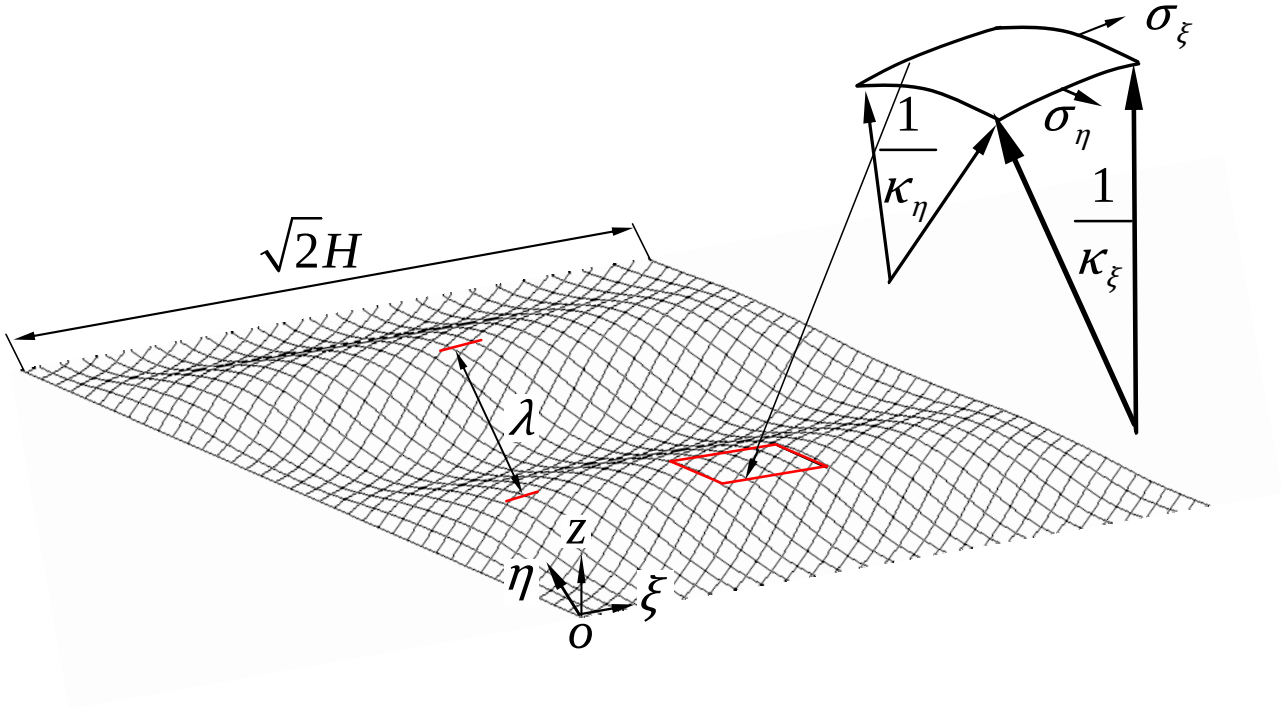

Fig. 4 Partial view of a single wrinkle strip

The conditions on out-of-plane displacementω are satisfied if the mode shape is assumed as[31]:

$$\omega = A\sin\frac{\pi\xi}{\sqrt{2}H}\sin\frac{2\pi\eta}{\lambda} \quad (1)$$

where$A$ and λ are amplitude and wavelength, respectively.

Based on Euler's formula, stresses in $\xi$and ηdirections can be obtained as follows:

$$\begin{cases} \sigma_\eta = -\dfrac{\pi^2 E t^2}{3(1-\nu^2)\lambda^2} \\ \sigma_\xi = E\dfrac{\gamma}{2} \end{cases} \quad (2)$$

where$\gamma=\delta/H$, according to the stress state of equilibrium, the followingequation can be established:

$$\sigma_\eta\kappa_\eta + \sigma_\xi\kappa_\xi = 0 \quad (3)$$

where$\kappa_\eta$and $\kappa_\xi$are curvatures of η andξdirections, respectively, and can be determined by following formulas:

$$\begin{cases} \kappa_{\xi} = \dfrac{\pi^2 A}{2H^2} \sin\dfrac{\pi\xi}{\sqrt{2}H} \sin\dfrac{2\pi\eta}{\lambda} \\ \kappa_{\eta} = \dfrac{4\pi^2 A}{\lambda^2} \sin\dfrac{\pi\xi}{\sqrt{2}H} \sin\dfrac{2\pi\eta}{\lambda} \end{cases} \quad (4)$$

Substituting Eqs. (2)and (4) into Eq. (3), simplifying and rearranging yields for the wrinkle wavelength the expression:

$$\lambda = 2\left[\frac{\pi^2 H^2 t^2}{3\gamma(1-\nu^2)}\right]^{0.25} \quad (5)$$

To find a reasonable expression for the amplitude *A* of the wrinkle, the imposed strain can be given by:

$$\varepsilon_{\eta} = -\frac{\gamma}{2} \quad (6)$$

Besides, the sum of the materials strain is given as follows:

$$\varepsilon_{\eta M} = -\frac{v}{E}\sigma_{\xi} \quad (7)$$

Average geometric strain is determined by:

$$\varepsilon_{\eta G} = -\frac{\pi^2 A^2}{\lambda^2} \quad (8)$$

According to relationship of geometric strain, we can obtain,

$$\varepsilon_{\eta} = \varepsilon_{\eta M} + \varepsilon_{\eta G} \quad (9)$$

Substituting Eqs. (6), (7) and (8) into Eq.(9), the expression of amplitude can be given as:

$$A = \frac{\sqrt{2(1-v)\gamma}}{2\pi}\lambda \quad (10)$$

3. Results and discussion

A rectangular monolayer h-BN sheet with a length of 14.94nm and a width of 4.93 nm is firstly considered in the study. When the upper side of the h-BN sheet subject to in plane shear displace in *x* position direction, the entire system starts to deform and bend to the right. The lateral displacement of different layers in *y* direction is proportional to the distance between the layer and

the bottom side. After the in plane shear displacement reaches up to the critical buckling value (0.08 nm), the wrinkles start to initiate on both free sides of the h-BN sheet, while the central region of the sheet keeps flat (shown in Fig.5a). To better observe this phenomenon, the out of displacementω of section S-S(shown in Fig. 1)is provided in Fig. 6a. Due to energy minimization of the monolayer sheet, the free edges are not kept flat, and generally have several ripples.This is in agreement with the results in graphene wrinkling analysesobtained by Duan [28]. Thus, the curve of the cross section view in Fig. 6a is asymmetric.With the increase of the shear displacement, the wrinkles spread to the central region. The wrinkling pattern of the monolayer h-BN sheet under the shear displacement of 0.12 nm is shown in Fig. 5b, and the cross section curve is plotted in Fig. 6b. When the shear displacement is further increased (δ=0.80 nm), the wrinkling pattern becomes almost uniform in the central region of the entire monolayer h-BN sheet as shown in Fig. 5c, and the crests and troughs are nearly identical with each other (shown in Fig.6c). The wrinkles geometric pattern consists of two parts: a general parallelogram of wrinkles with uniform crests in the central regionand two triangular slack regions, which contain a small highly stressed corner and a triangular slack region, near the side edges. The uniform crests in that general parallelogram are found to be parallel to each other with an angle of 45°separated from the load direction. Those wrinkles are attributed to shear displacement, and indicating that the angle between the tensile stress plane of wrinkles and load direction equals to 45°. Compared Fig. 6d with Fig. 6c, it is noted that the number of wrinkling will increase with the increasing of the shear displacement.The influence of the shear displacement on the wrinkles number is shown in Fig.7. It can be seen that when the shear displacement is gradually increased, the number of wrinkling including crests and troughs changes suddenly, which is due to mode jump in the buckling membrane[32].

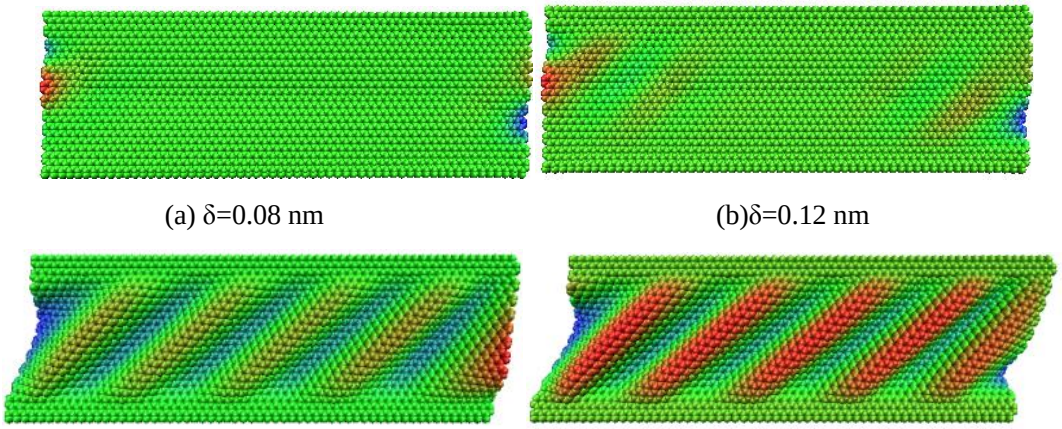

(a) δ=0.08 nm (b)δ=0.12 nm

(c)δ=0.80 nm (d)δ=1.20 nm

Fig. 5Wrinkling pattern of monolayer h-BN sheet

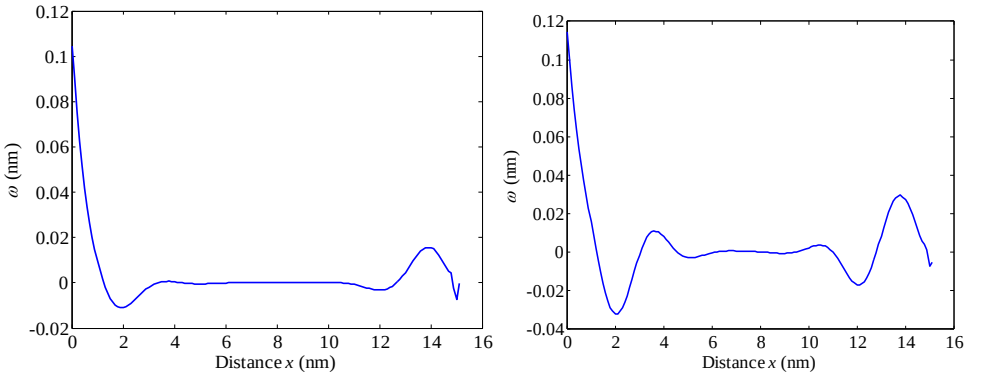

(a) δ=0.08 nm (b)δ=0.12 nm

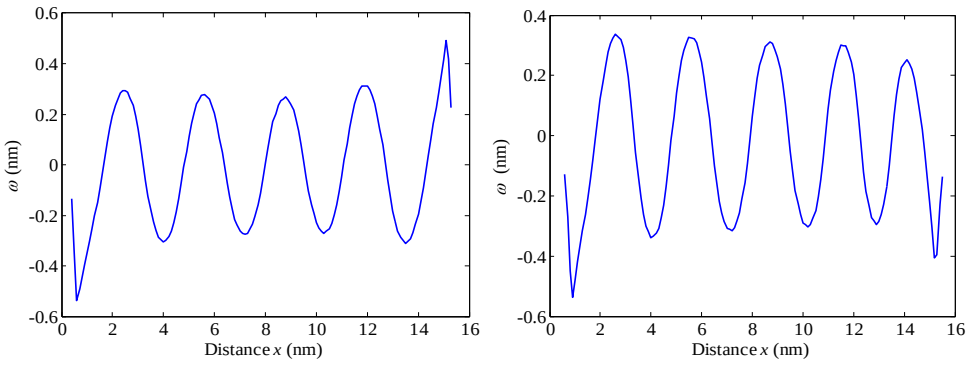

(c)δ=0.80 nm (d)δ=1.20 nm

Fig. 6Cross section profile of monolayer h-BN sheet

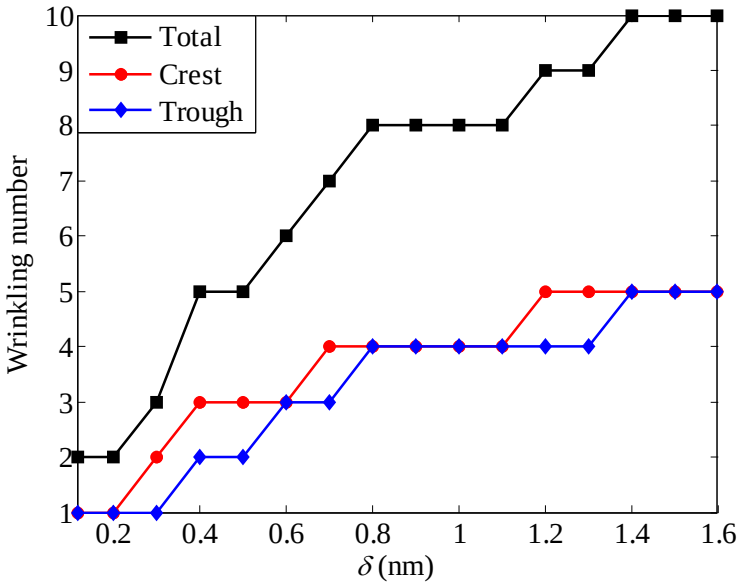

Fig. 7 Variation of wrinkling number with the shear displacement

3.1.Wrinkle shape

From the analytical analysis, it is known that$\xi$and $\eta$are the tensile and the compressive directions of wrinkles, respectively. The wrinkle amplitudes are different in the free layer, and the maximum amplitude is expected to occur at the middle between the fixed and moving edges of the h-BN sheet. In order to validate the computational analyses and to examine the longitudinal shape of a wrinkle, the amplitudes of a number of profiles of the sheethave been measured at the following distance from the bottom fixed edge, y=0.5, 1.0, 1.5, 2.0, 2.5, 3.0, 3.5, 4.0, 4.5 nm, for the same shear displacement. Now we define a new coordinate axisη', shown in Fig. 1,whose positive direction is parallel to the opposite direction ofηaxis, the point (0, 4.93) is the origin of the new axis. The amplitudes of these wrinkles have been plotted in Fig. 8 together with a half sine wave whose amplitude has been scaled to match the maximum amplitude. It is noted that the wrinkle shapesin longitudinal direction can be in good agreement with the simple sinusoidal modeshape. The amplitude remains zeroon the edges due to the fixed constrains, and reaches to the maximum value in the middle between the fixed and moving edges. This result is in agreement with the conclusion drawn by Won [31].

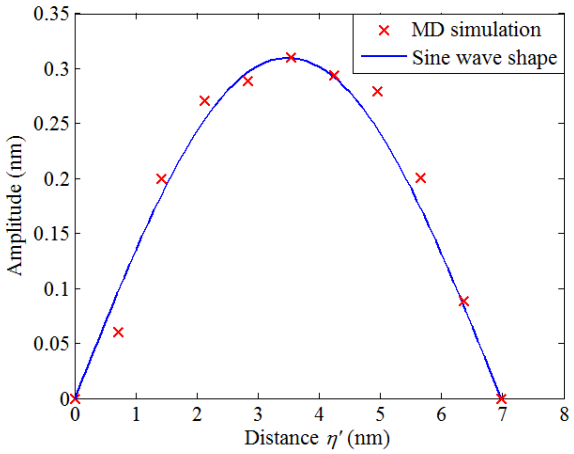

Fig.8 Comparison of the wrinkle shape with a sinusoidal mode shape

3.2.Amplitude and wavelength

As mentioned previously, the amplitude of the wrinkle obeys the sinusoidal mode shape in longitudinal direction, thus the average amplitude is adopted to evaluate the effects of the shear displacement on this parameter. Since the wavelength of the wrinkle can be seen to remain approximately constant, expect near the fixed and moving edges due to the localized deformation imposed by the fixed constrains. Thus, the wavelength can be considered to be uniform in the longitudinal direction under the same shear displacement.In order to investigate the effects of the shear displacement on the winkle profile in terms of amplitude and wavelength, the average amplitude and wavelength of the monolayer h-BN sheet with a length of 14.94nm and a width of 4.93nm subjected to shear displacement are plotted in Fig. 9.It indicates that the average amplitude increases with the increasing shear displacement. After the shear displacement reaches 1.2 nm, the amplitude approximatelyremains constant at around 0.218 nm, as shown in Fig. 9a. On the contrary, the wavelength decreases with the increasing shear displacement, and when the shear displacement is higher than 1.35 nm, the wavelength becomes constant as shown in Fig. 9b.The theoretical computational results based on Eqs (5) and (10) are also plotted in Fig.9. It is noted that the theoretical model for wavelength can be in good agreement with the MD simulation, while the analytical model for amplitude can only provide the reasonable estimation at some intervals of shear

displacement. Since the shape and size of the sheet will affect the computational accuracy of Eqs. (5) and (10) based on a continuum model, three monolayer h-BN sheets with different aspect ratios have been utilized to explore the geometric influences. Table 1 shows the result comparison between MD simulations and theoretical computations. It can be seen that the discrepancies are less than 30%, and the theoretical models can be utilized to provide an acceptable estimation for the wrinkle profile of monolayer h-BN sheets.

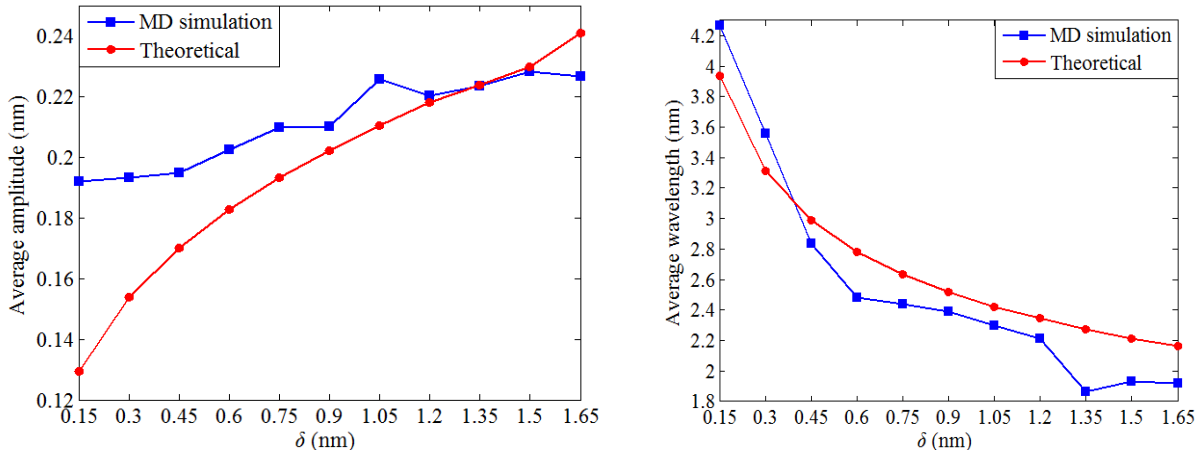

(a) Amplitude vs. shear displacement (b) Wavelength vs. shear displacement

Fig. 9Influences of shear displacement on winkle profile

Table. 1 Comparison of average amplitudeand wavelength between MD simulation and theoreticalcalculation

Length/Width (L/H)	Shear displacement (nm)	Wavelength(nm)			Amplitude(nm)		
		MD	Eq.(5)	Difference (%)	MD	Eq.(10)	Difference (%)
14.94/7.39=2:1	0.5	3.52	3.30	-6.7	0.18	0.16	-12.5
	1.0	2.81	3.32	15.4	0.19	0.23	17.4
	1.5	2.58	3.01	14.28	0.22	0.26	15.4
14.94/4.93=3:1	0.3	3.56	3.31	-10.3	0.19	0.15	-26.7
	0.6	2.48	2.78	10.7	0.20	0.18	-11.1
	1.2	2.21	2.34	5.6	0.22	0.21	-4.8
14.94/9.93=3:2	1.0	3.04	4.15	26.7	0.22	0.25	12
	2.0	2.76	3.49	20.9	0.28	0.29	3.4
	3.0	2.33	3.15	25.9	0.29	0.32	9.4

3.3. Potential energy

Due to ultra thin thickness, the h-BNsheet has the enough freedoms to release the in-plane

compressed shear energy to form the wrinkles, and the compressed shear energy can be released by moving out of plane of the B and N atoms and further to form wrinkles. Taking the monolayer h-BN sheet with a length of 14.94nm and a width of 4.93nmas an example, the length of B-N bond increases with the increasing of the shear displacement, and then the wrinkling phenomenon happens to release the potential energy. The wrinkling patterns of the monolayer h-BN sheet under shear displacement have been discussed previously. In this section, the potential energy is examined to obtain further insight into the wrinkling behavior of such kinds of h-BN sheets. As shown in Fig. 10, the potential energy quadraticallyincreases with the increasing shear displacement until the failure shear displacement of δ_r=1.69 nm.When the shear displacementis higher thanδ_r, there are small drops in energy indicating that energy release due to the breaking of B-N bonds. Meanwhile, the structural integrity of the h-BN sheet has been destroyed. Besides undergoing a successive breaking of B-N bonds, the h-BN sheet also experiences a successive rearrangement of B-N bonds, which can reasonably explain amounts of small increases and small drops in energy. It is also noted that that the initial breaking of B-N bond often occurs in the top right cornerand the energy curve will have a drop as shown at the point D. After that, theB-N bond breaking happens in bottom left corneras demonstrated at the point E. For a clear understanding of this, the energy at points A, B and C (shown in Fig. 1) have been investigated and plotted in Fig.11.It is noted that the energies of the three points are almost identical at the beginning of the shear displacement. However, the energy of point B increase faster than that of point C, and thus point B reaches to the failure stress firstly and then point C. The energy of point increase slower than those of points B and C, and the maximum value of the energy of point Ais lower than those of other points due to the energy release for the fractures at points B and C. From the energy distribution (Fig. 12), it is also demonstrated that the energies in the two corners aresignificantly higher than other sections. The influences of the

geometric parameters on the potential energy have also been provided in Fig. 10. It is noted that the critical potential energy decrease with the increasing width H. This is in good agreement with the analytical prediction, since the potential energy *U*can be given as follows [31]:

$$U = \frac{(1-\nu)Et\gamma}{2}\left(\frac{\pi^2 t^2}{6(1-\nu^2)\lambda^2}+\frac{\gamma\lambda^2}{32H^2}\right). \quad (11)$$

It can be seen that the increased width H can reduce the critical potential energy. However, the aspect ratio of the h-BN sheet has slightly influences on the wrinkling patterns.

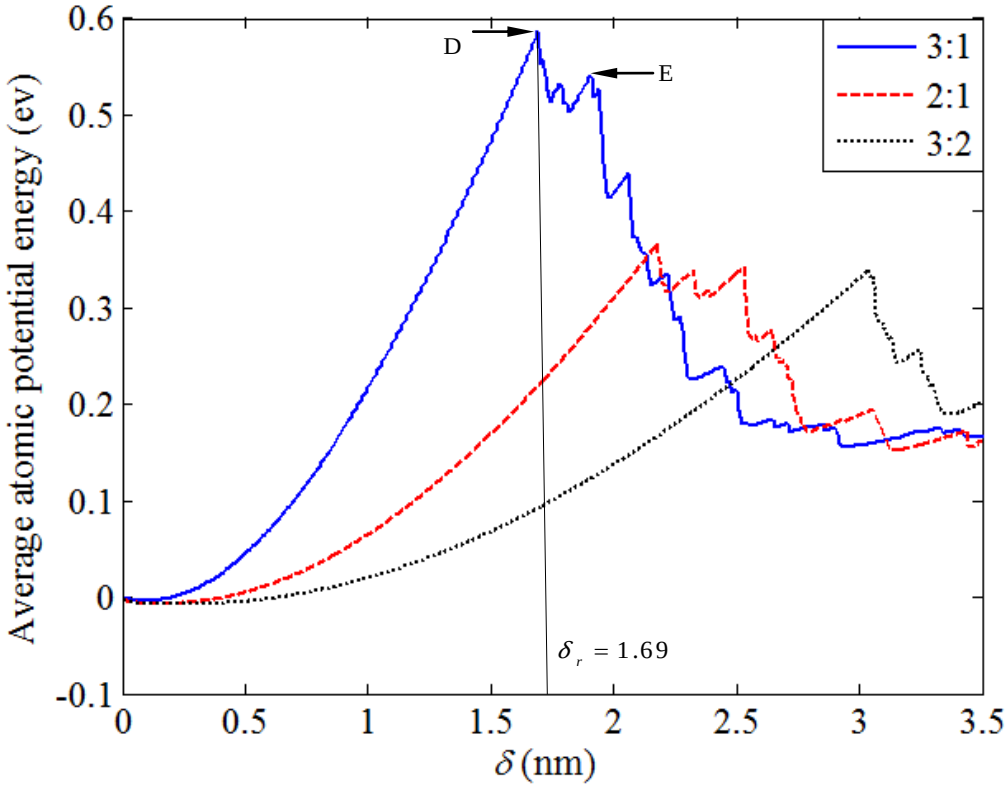

Fig. 10 The variations of potential energy of the h-BN sheets with shear displacement

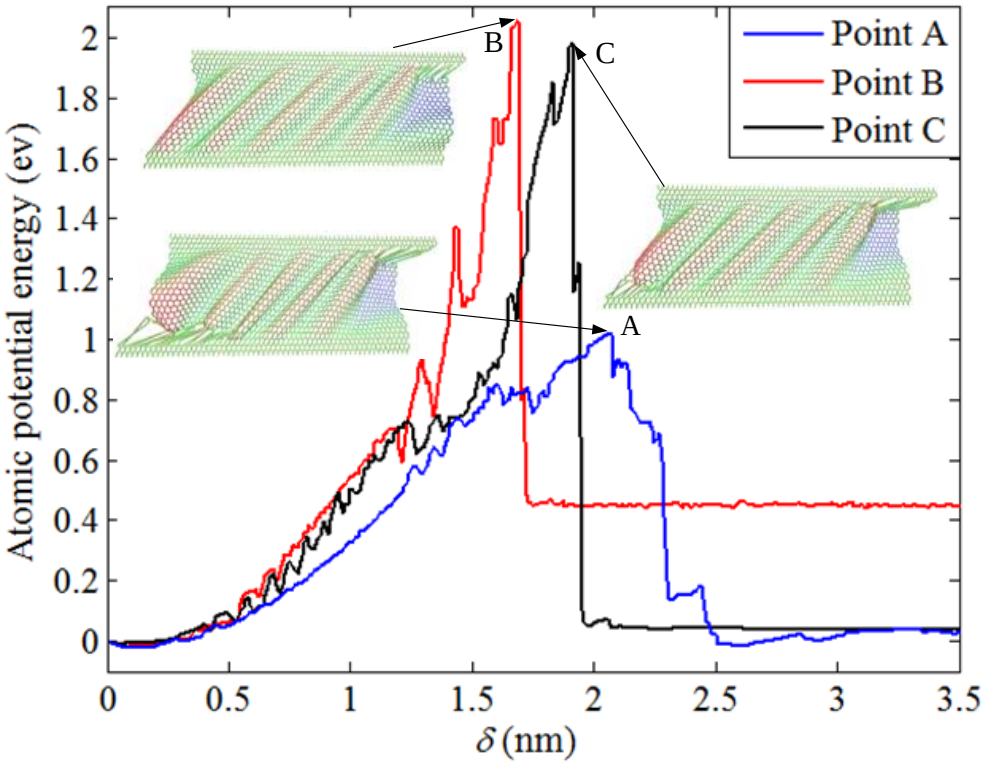

Fig. 11The variations of potential energy of atoms at points A, B and C

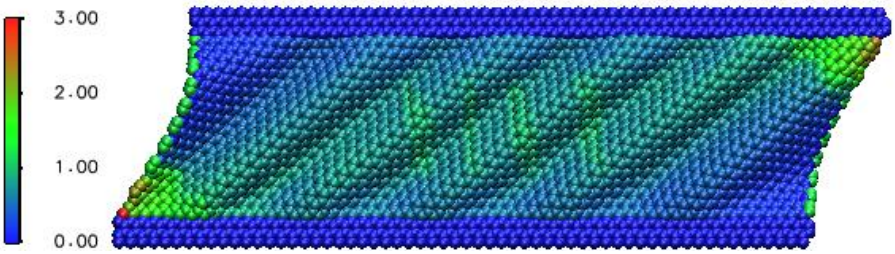

Fig. 12 Energy distribution of the h-BN sheet (δ_t=1.69 nm)

3.4. Stress

To obtain further insights into the wrinkling mechanism, the stress in the monolayer h-BN sheet must be explored. As shown in Fig. 4, the stress can be divided into compressive stress and tensile stress in ξ and η directions, respectively.It is recognized that the compressive stress is the main reason to form wrinkles. The h-BN sheet can generate wrinkling pattern even subjected to a small compressive stress due to the relatively low bending rigidity. The compressive and tensile stresses of the monolayer h-BN sheet with the length of 14.94nm and the width of 4.93nm are shown in Fig. 13. It is noted that the value of compressive stress is much smaller than that of tensile

stress.At the initial shear displacement (less than 0.1 nm), both compressive and tensile stresses increase with the increasing shear displacement. Then the compressive stress almost keeps constant, while the tensile stress increases quickly until the fracture shear displacement. After fracture point, the tensile stress has several drops due to the B-N bond breaking, and the compressive stress has a slight drop around the fracture point and then return back to previous constant value. The tensile stress can affect the fracture, and the compressive stress control the wrinkle deformation instead.The tensile stresses of the monolayer h-BN sheet with different aspect ratios have been shown in Fig. 14. It is noted that the fracture stress reduce with the increasing of width H. There are several sudden drops corresponding to the energy releases in Fig. 11. Based on Eq. (2), tensile stress only depends on size of *H*, and is inverse proportional to *H*.The local stresses on points A, B and C are shown in Fig. 15. It can be seen that the local stresses are almost identical and increase with the increasing shear displacement. However, the local stress on point B firstly reaches up to the fracture stress and has a sudden drop, and then the stress on point C raises to the fracture stress and drop down to a small value. Since there is no fracture at point A, the stress on point A slowly drops to a certain value due to the fracture on points B and C.

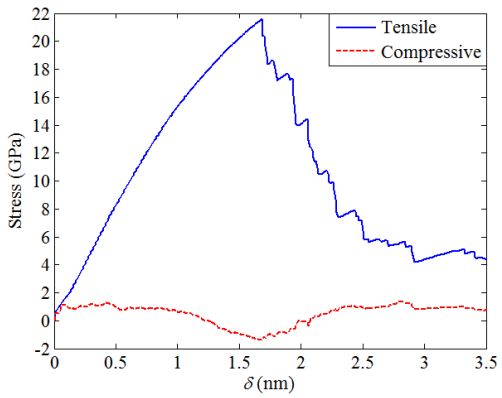

Fig. 13Variations of average stress of atoms with the shear displacement

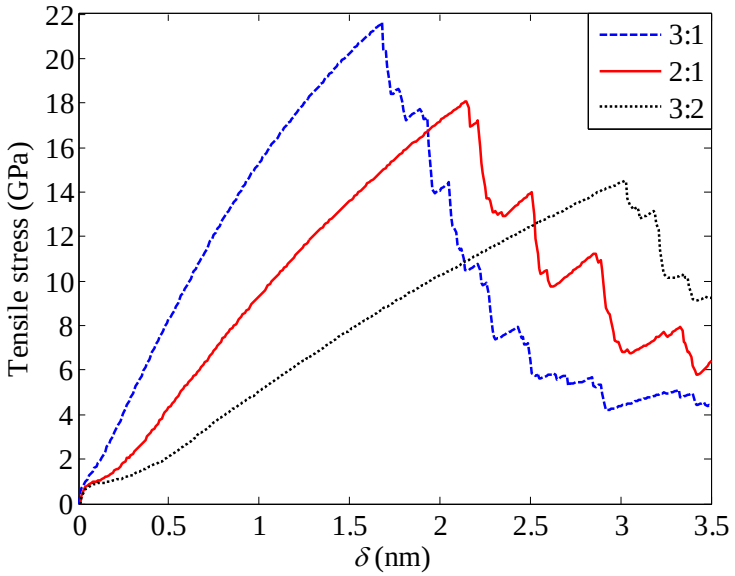

Fig. 14Variations of average stress of atoms with the shear displacement forthree h-BN sheets with different aspect ratios

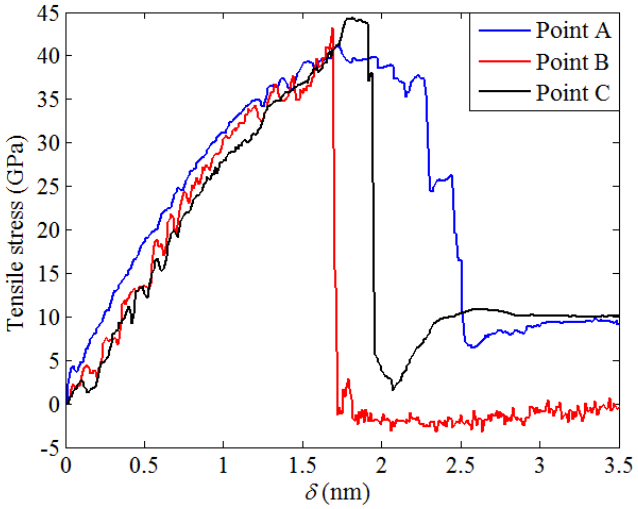

Fig.15Variations of tensile stress of atoms at the points A, B and C with the shear displacement

3.5.Edge effect

It is well known that the mechanical property of the monolayer h-BN sheet is anisotropy due to the chirality of the structure. The shear displacement in zigzag and armchair directions are utilized to explore the edge effects on the shear properties of the monolayer h-BN sheets. It is noted that the edges have little effects on the wrinkling patterns, butsignificantly influences the fracture behaviors. Thus, the potential energy and stress are measured and plotted in Fig. 16.It can be seen that the curves for energy and stress are almost identical before the fracture happen in the h-BN sheet subjected to shear displacement in zigzag direction. The h-BN sheet can bear larger shear

displacement in armchair direction than that in zigzag direction. Furthermore, the temperature effects on the failure shear displacement and failure tensile stress are also examined using the MD simulation. The computational results are shown in Fig. 17. It is noted that the failure shear displacement and failure tensile stress reduce with the increasing temperature for both shear load directions. The fracture stress in armchair direction is larger than that in zigzag directionin lower temperature (less than 800K), and on the contrary in higher temperature.However, the failure shear displacement changes at temperature of 1300K. This is mainly due to the chirality of the h-BN sheet.

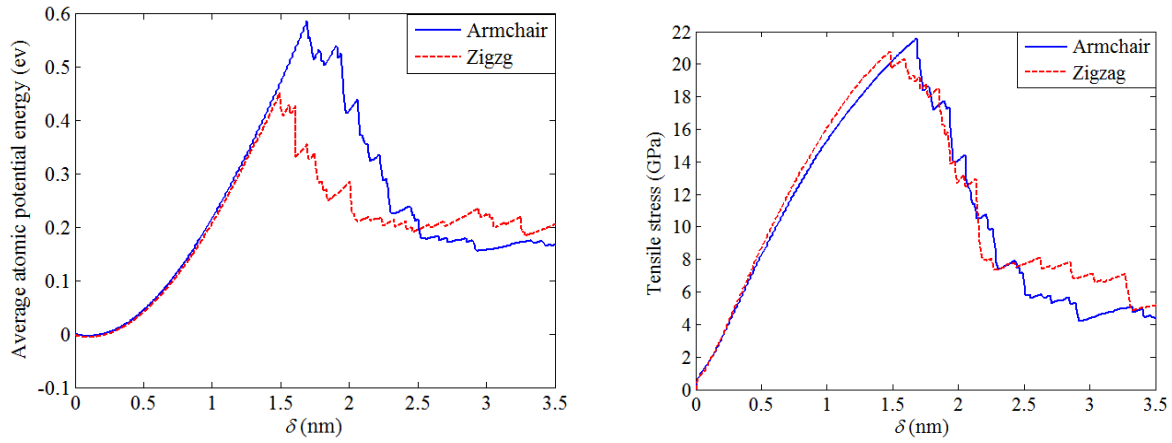

(a) Energy (b) Stress

Fig. 16Edge effect on fracture of h-BN sheets

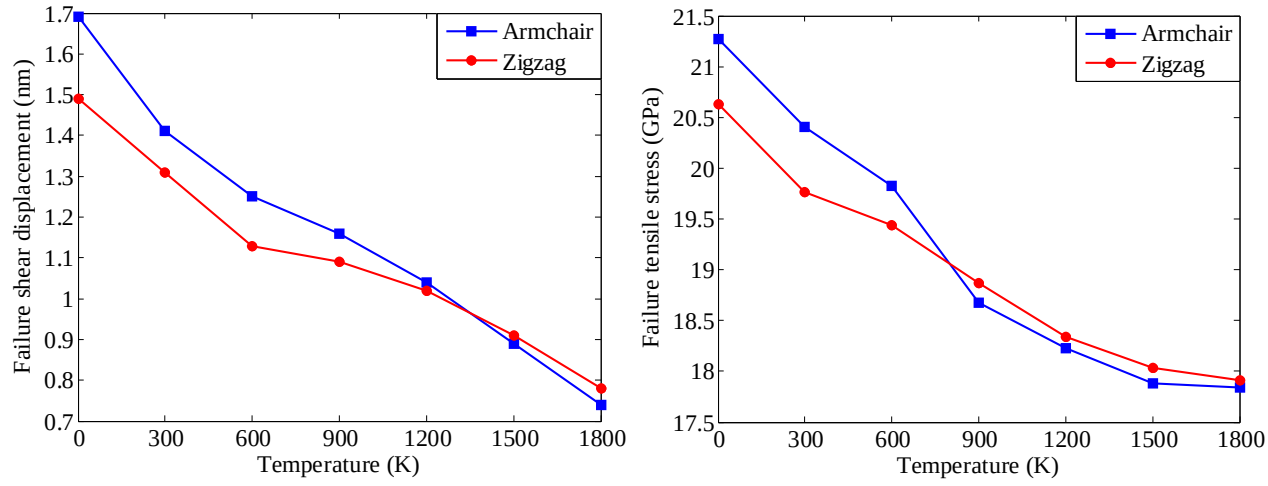

(a) Failure shear displacement (b)Failure tensile stress

Fig. 17 Temperature effects on failure of h-BN sheet

4. Conclusions

The mechanical properties including wrinkling patterns and fracture behavior of the monolayer h-BN sheets have been investigated using classic molecular dynamics simulations and continuum model. Based on the established computational model and methodology, extensive simulations have been carried out to study the mechanical characteristics of the monolayer h-BN sheet. The achieved results can provide the advanced knowledge of h-BN sheets for their potential applications.

When the monolayer h-BN sheet is subjected to shear displacement, the wrinkles start initially at the two free side edges, and then spread to the central region. The wrinkling shape in longitudinal direction can be modelledby a simple sinusoidal mode shape. The average wrinkling amplitude increases with increasing shear displacement, however, the wrinkling wavelength decreases with the increasing shear displacement, and correspondingly the wrinkling number increases with a sudden jump mode.

The average potential energy quadraticallyincreases with the increasing shear displacement until top right corner of h-BN sheet is broken. After fracture occurrence, the energy dropssuddenly due to the B-N bond breaking. The average stress also increases with the increasing shear displacement and drops after the fracture of the h-BN sheet.The compressive stress almost remains constant, and is smaller than the tensile stress. It is observed that the compressive stress control the wrinkling phenomenon and tensile stress dominates the fracture.The fracture tensile stress is inverse proportional to the width of h-BN sheet.In addition, the fracture tensile stress varies in different edge directions due to the anisotropic property. The fracture stress in armchair direction is larger than that in zigzag directionin lower temperature and larger in higher temperature. However, the increasing temperature can generally reduce the fracture tensile stress in both directions.

Acknowledgements

This research is supported by National Natural Science Foundation of China (No. 51175372), Reserved Academic Program of Peiyang Scholar, and Program for New Century Excellent Talents in University (No. NCET-11-0374).

References

[1] K.S.Novoselov,D.Jiang,F. Schedin,T.J. Booth,V.V. Khotkevich,S.V. Morozov,et al., Two-dimensional atomic crystals,Proceedings of the National Academy of Sciences of the United States of America,2005,102(30):10421-10423.

[2] O. Dubay, G. Kresse, Accurate density functional calculations for the phonon dispersion relations of graphite layer and carbon nanotubes, Physical ReviewB, 2003,67(3):035401.

[3] G. Kern, G. Kresse,J. Hafner, Ab initio calculation of the lattice dynamics and phase diagram of boron nitride,Physical Review B, 1999, 59(13):8551-8559.

[4] A. Pakdel, C. Zhi, Y. Bando, D. Golberg, Low-dimensional boron nitride nanomaterials, Materials Today, 2012, 15(6): 256-265.

[5] Z.L. Hou, M.S. Cao, J. Yuan, X.Y. Xiao, X.L. Shi, High-temperature conductance loss dominated defect level in h-BN: Experiments and first principles calculation,Journal of Applied Physics, 2009, 105(7): 076103-076103-3.

[6] J. Zhou, Q. Wang, Q. Sun, P. Jena, Electronic and magnetic properties of a BN sheet decorated with hydrogen and fluorine, Physical Review B, 2010, 81(8): 085442-085442-7.

[7] Z. Zhang, W. Guo, B.I. Yakobson, Self-modulated band gap in boron nitride nanoribbons and hydrogengated sheets, Nanoscale, 2013, 5(14): 6381-6387.

[8] G.W. Rowe, Some observation on the frictional behavior of boron nitride and of graphite, Wear, 1960, 3(4): 274-285.

[9] R.F. Deacon, J.F. Goodman, Lubrication by lamellar solids, Proceedings of the Royal Society of London A, 1958, 243(1235): 464-482.

[10] A.J. Haltner, Sliding behavior of some layer lattice compounds in ultrahigh vacuum, Tribology, 1966, 9(2): 136-148.

[11] J. Yu, L. Qin, Y.F. Hao, S.Y. Kuang, X.D. Bai, Y.M. Chong, et al., Vertically aligned boron nitride nanosheets: chemical vapor synthesis, ultraviolet light emission, and superhydrophobocity, ACS Nano, 2010, 4(1): 414-422.

[12] A.A. Peyghan, M. Noei, S. Yourdkhani, Al-doped graphene-like BN nanosheet as a sensor for

para-nitrophenol: DFT study, Superlattices and Microstructures, 2013, 599(33): 115-122.

[13] Y. Kimura, T. Wakabayashi, K. Okada, T. Wada, H. Nishikawa, Boron nitride as a lubricant additive, Wear, 1999, 232(2): 199-206.

[14] B. Chen, Q. Bi, J. Yang, Y. Xia, J. Hao, Tribological properties of solid lubricants (graphite, h-BN) for Cu-based P/M friction composites, Tribology International, 2008, 41(2): 1145-1152.

[15] L. Song, L.J. Ci, H. Lu, P. B.Sorokin, C.H. Jin, J. Ni, et al., Large scale growth and characterization of atomic hexagonal boron nitride layers, Nano Letters, 2010, 10(8): 3209-3215.

[16] H. Yabu, M. Shimomura, Single-step fabrication of transparent superhydrophobic porous polymer films, Chem. Mater., 2005,17(21):5231-5234.

[17] A. Pakdel, C. Zhi, Y. Bando, T. Nakayama, D. Golberg, A comprehensive analysis of the CVD growth and boron nitride nanotubes, Nanotechnology, 2012, 23(21):215601-215606.

[18] L.H. Li, Y. Chen, Superhydrophobic properties of nonaligned boron nitride nanotube films, Langmuir, 20120,26(7):5135-5140.

[19] L.B. Boinovich, A.M.Emelyanenko, A.S.Pashinin, C.H. Lee, J. Drelich, Y.K. Yap, Originsof thermodynamically stable superhydrophobicity of boron nitride nanotubes of coating, Langmuir, 2012, 28(2):1206-1216.

[20] A.D. Aliev, L.B. Boinovich, V.L. Bukhovets, A.M. Emelyanenko, A.M. Gorbunov, A.E. Gorodetskii, et al., Superhydrophobic coatings based on boron nitride nanotubes: the mechanism of Superhydrophobicity and self-regeneration of highly hydrophobic properties,Nanotechnologies in Russia, 2011,6(11):723-732.

[21] W. Lei,D. Portehault, D. Liu, S. Qin, Y. Chen, Porous boron nitride nanosheets for effective water cleaning, Nature Communications, 2013, 4(2):1777-1783.

[22] J.C. Meyer, A.K.Geim, M.I. Katsnelson, K.S. Novoselov, T.J. Booth, S.Roth, Thestructureof suspended graphene sheets, Nature, 2007,446(7131):60-63.

[23] K.H. Kim, Y. Oh,M.F. Islam, Graphene coating makes carbon nanotube aerogels superelastic and resistant to fatigue,Nature Nanotechnology, 2012,7(9):562-566.

[24] V.B. Shenoy, C.D. Reddy, Y.Z. Zhang, Spontaneous curling of graphene sheets with reconstructed edges, ASC Nano, 2010, 4(8): 4840-4844.

[25] K.Kim, Z. Lee, B.D. Malone, K.T. Chan,B. Aleman,W. Regan,et al., Multiply folded graphene, Physical Review B, 2011,83(24):245433-245440.

[26] C.Y. Wang, K. Mylyaganam, L.C. Zhang, Wrinkling of monolayer graphene: A study by molecular dynamics and continuum plate theory, Physical Review B, 2009, 80(15): 155445-155449.

[27] W. Bao,F. Miao,Z.Chen,H.Zhang,W. Jang,C. Dames, et al., Controlled ripple texturing of suspended graphene and ultra-thin graphite membranes, Nature Nanotechnology, 2009, 4(9): 562-566.

[28] W.H. Duan, K. Gong, Q. Wang, Controlling the formation of wrinkles in a single layer graphene sheet subjected to in-plane shear, Carbon, 2011, 49(9): 3107-3112.

[29] Z. Zhang, W.H. Duan, C.M. Wang, Tunable wrinkling pattern in annular graphene under circular shearing at inner edge, Nanoscale, 2012, 4(16), 5077-5081.

[30] T. Enoki, S. Fujii, K. Takai, Zigzag and armchair edges in graphene, Carbon, 2012, 50(9):3141-3145.

[31] Y.W. Wong, S.Pellegrino, Wrinkled membranes, Part II:analytical models, Journal of Mechanics of Materials and Structures, 2006,1(1):27-62.

[32] Y.W. Wong, S. Pellegrino, Wrinkled membranes, Part III:numerical simulations, Journal of Mechanics of Materials and Structures, 2006,1(1):63-95.